



HAL
open science

Comparing results of a power prediction tool with measured data from a series of 35 boats

Charles Dumortier, Jean-François Bonnet, Nicolas Régnier, Yves Ousten

► To cite this version:

Charles Dumortier, Jean-François Bonnet, Nicolas Régnier, Yves Ousten. Comparing results of a power prediction tool with measured data from a series of 35 boats. *Ocean Engineering*, 2019, 178, pp.501-516. 10.1016/j.oceaneng.2018.12.076 . hal-02120784

HAL Id: hal-02120784

<https://hal.science/hal-02120784>

Submitted on 22 Oct 2021

HAL is a multi-disciplinary open access archive for the deposit and dissemination of scientific research documents, whether they are published or not. The documents may come from teaching and research institutions in France or abroad, or from public or private research centers.

L'archive ouverte pluridisciplinaire **HAL**, est destinée au dépôt et à la diffusion de documents scientifiques de niveau recherche, publiés ou non, émanant des établissements d'enseignement et de recherche français ou étrangers, des laboratoires publics ou privés.



Distributed under a Creative Commons Attribution - NonCommercial 4.0 International License

COMPARING RESULTS OF A POWER PREDICTION TOOL WITH MEASURED DATA FROM A SERIES OF 35

BOATS

1

2 Charles DUMORTIER¹, Jean-François BONNET², Nicolas REGNIER², Yves OUSTEN³

3 ¹ CNC Couach, Rue de l'Yser, 33470 Gujan-Mestras France, French shipyard / University of Bordeaux /
4 charles.dumortier@u-bordeaux.fr

5 ² I2M (Institute of Mechanical and engineering) / ³IMS (Laboratory of the integration of the material into the system)

6

7

I. ABSTRACT

8 Power prediction is one of the major steps when it comes to design a military boat. Having a fast running and
9 reliable tool to select the appropriate couple engine/propulsion permits to explore more hull's possibilities.

10 This study is built on a comparison made between a predictive tool and a series of 35 hard chine planing boats,
11 constructed to be identical. The different theories used to program the Power Prediction Tool (PPT) will be cited
12 as reference but will not be developed.

13 In this article, we present the influence of the different parameters and the validity of our tool.

14

15

II. KEYWORDS

16 Vessel power prediction; Real boat power measurement; Ship operational performance; Manufactured boat
17 series; Improvement of Savitsky theory.

18

III. NOMENCLATURE

Symbol	Units	Description	Symbol	Units	Description
OPC	-	Efficiency of the propulsive system	D_{aero}	m	Boat aerodynamic drag
OPC'	-	Efficiency of both gearbox and propulsive system	$C_{p_{aero}}$	m	Distance between D_{aero} and CG measured normal to D_{aero}
η_{meca}	-	Efficiency of the gearbox	m	kg	Boat mass
P	kW	Engine power	g	$m.s^{-2}$	Acceleration of gravity
v	$m.s^{-1}$	Boat speed	N	N	Hydrodynamic force normal to the bottom
Rt	N	Total resistance of the boat	c	m	Distance between N and CG, measured normal to N
VCG	m	Vertical position of the center of gravity (origin at boat transom)	ϵ	°	Inclination of thrust line relative to keel line
LCG	m	Longitudinal position of the center of gravity (origin at boat transom)	T	N	Propeller thrust
$P_{measured}$	kW	Absorbed power measured during tests	f	m	Distance between T and CG measured normal to T
$P_{calculated}$	kW	Absorbed power calculated with the program	D_f	N	Frictional drag component along the bottom surface
P_{max}	kW	Nominal power of the engine (1192kW for this study)	a	m	Distance between D_f and CG measured normal to D_f
ρ_{air}	$kg.m^{-3}$	Air density	M	Nm	Total pitching moment
Cx	-	Boat's aerodynamic drag coefficient	LOA	m	Boat length overall
S_{house}	m^2	Frontal surface of the wheelhouse	F_v		Volumic Froude number
S_{hull}	m^2	Frontal surface of the hull	L_p	m	Projected length of the chine
S_{boat}	m^2	Frontal surface of the boat	P_{jet}	W	Jet absorbed power
τ	°	Boat trim	B_{px}	m	Maximum chine beam excluding external spray rail
BSS	m	Breadth of wheelhouse	D	m	Boat draft
HSS	m	Height of wheelhouse	E	%	Difference between measured and computed power divided by maximum engine power
DBH	m	Distance between bow and wheelhouse	H_{hull}	m	Hull height
B_{max}	m	Hull width			

IV. INTRODUCTION

21 Energy use in naval operation is a growing concern (Turan, 2015), due to high energy prices and
 22 environmental awareness. While solutions for freight transport have long been studied (Lu et al, 2015; Cichowicz
 23 et al, 2015), the case of yachting and of light military ships is far less documented. For these vessels, significant
 24 potential energy savings can be found in hull design, engine design, air conditioning and onboard equipment
 25 energy efficiency. The current paper focuses on hull design and its influence on engine power and energy
 26 consumption. Hull design requires a preliminary design phase, using a complete set of data on geometrical
 27 elements and ship weight. In this paper, a power prediction tool (PPT) has been developed for preliminary design

28 and tested on a series of 35 boats. Due to construction techniques, slight differences in weight, weight distribution
29 and engine power performances can be found in the ship series¹. The goal of the paper is to exploit measured data
30 (weight, speed, engine power) to develop, validate and improve the power prediction tool (PPT).

31 The purpose of the PPT is to:

- 32 -be trustable
- 33 -be easy to use and rapid to calculate.
- 34 -study the general picture of the boat
- 35 -be used to reduce CFD computation time

36 Indeed with the same computing power, calculating the boat drag with the PPT is more than ten thousand time
37 faster than using a CFD code. Where few seconds are required to compute more than fifty speed steps with the
38 PPT, a CFD code needs several hours to compute the drag for only one speed step. This advantage makes the PPT
39 an efficient tool for the preliminary design work (variation of the general parameters of the hull). Additionally it
40 can be used to reduce the CFD computation time. Using PPT outputs' such as trim and boat draft as CFD inputs'
41 helps to position the boat close to his equilibrium position.

42 However the PPT is not intended to replace a CFD software. It can be seen as a preliminary tool used to give
43 quick answers and orientations on hull geometry. Then the CFD tool can be used to optimize the hull shape.

44 On the one hand, it is true that setting up the simulation can be very complex, time consuming and running the
45 code requires an important calculation power and/or an important amount of time to give some results (**Tezdogan**
46 **et al, 2015; Caponnetto**). But on the other hand a CFD code is extremely powerful to study all the geometrical
47 details of the hull such as rudder blade tips, keel shape, water inlets, air inlets ...

48 The PPT is mainly based on Savitsky theory. Some modifications have been done to improve its precision at
49 low speed and the aerodynamic drag is treated unconventionally. These modifications have been validated with
50 data extracted from real boats and from towing tank tests.

51 Before comparing the PPT results with real boat measurements, its constitutive steps are detailed.

¹ See appendix 1 : PPT inputs variation range

52

V. PPT DESCRIPTION

53 The PPT is programmed on Excel and coded in VBA (Visual Basic for Applications) in order to easily build
54 a user friendly interface.

55 To best describes the program, **Figure 1** presents a screenshot of all inputs of the tool. Parameters in the hull
56 section are used to implement the Savitsky's equations (**Savitsky, 1964**) to calculated the boat's hydrodynamic
57 drag. Regarding the restriction of the procedure, Daniel Savitsky himself says: "*the foregoing procedures are*
58 *carried out for the entire speed range of interest (with the restriction that $C_v \geq 1,0$)*". C_v is called the speed
59 coefficient and is equal to $\frac{v}{\sqrt{gB}}$ with B the beam of the planning surface. Other limitation have been given by
60 (**Ekman et al, 2016**) at page 8 section "*Limitations and assumptions*"².

61 For the studied boat of this paper the C_v is higher than 1 for speed over than 12 knots.

62 Savitsky's equations can be implemented thanks to (**Savitsky, 1964**) and also by using the work of Svahn
63 (**Svahn, 2009**) but the original paper of Savitsky should be read. The only trick for this computational method
64 to be fully automatic, is to make a loop to calculate the trim. To make it, it is necessary to calculate what Svahn
65 names the "*pitching moment*", equation 35 in (**Savitsky, 1964**) and 2.29 in (**Svahn, 2009**):

$$M_{tot} = mg \left[\frac{c}{\cos \tau} (1 - \sin \tau \sin(\tau + \varepsilon)) - f \cdot \sin \tau \right] + D_f (a - f)$$

66
67 If this pitching moment is negative then all the Savitsky procedure should be started again from the beginning
68 with an higher value of the trim and if it is positive the guessed value of the trim should be smaller.

69 Once the hydrodynamic drag is known, it is multiplied by an empirical correction factor developed by
70 (**Blount, Fox, 1976**) called Mfactor:

$$\text{Mfactor} = 0.98 + 2 \left(\frac{LCG}{Bpx} \right)^{1.45} e^{-2(Fv - 0.85)} - 3 \left(\frac{LCG}{Bpx} \right) e^{-3(Fv - 0.85)}$$

71
72 It intends to correct the under prediction of the hump speed drag.

73 In addition to the drag prediction, what Angeli names "Critical trim" in (**Angeli, 1973**) is calculated by two
74 approaches:

² See appendix 2: Savitsky procedure limitations and assumptions given by Ekman et al, 2016

75 → equation 14 in (Angeli, 1973):

$$\tau_c^{4/3} = \frac{(106 + 85 \frac{B_T}{B_x}) (1 + 0.2 \frac{\beta_6 - \beta_{10}}{\beta_6}) (\frac{Y}{X})^{0.75}}{F_v^2 Y^2 f}$$

76

77 → equation developed by Lewandowski in the discussion section in (Celano, 1998):

$$\tau_{crit} = -1.87 + 12.54 \sqrt{\frac{C_L}{2}} + 80.87 \frac{C_L}{2} + 0.193\beta - 0.0017\beta^2 - 0.3125\beta \sqrt{\frac{C_L}{2}}$$

78

79 This parameter indicates the upper trim limits. A trim higher or equal to the Critical trim value presents a
80 high risk of porpoising. Two equations are used to compute it in order to be conservative. At each speed step,
81 the lower value resulting of the two equations is considered as the “Critical trim”.

82 In parallel of the hydrodynamic drag calculation, the aerodynamic drag need to be calculated. It is done by
83 using the inputs in the aero section of **Figure 1**. This calculation needs be done just before evaluating the boat
84 pitching moment. Indeed, the aerodynamic drag force modify the boat equilibrium. The original Savitsky
85 equation 35 has been modified to take the aerodynamical effects into account.

86 The general equation to calculate the aerodynamic drag (D_{aero}) of a solid is :

87 $D_{aero} = \frac{1}{2} \rho_{air} S C_x v^2$ where S is the frontal surface of the solid. (See Appendix 1 of (Savitsky, D.,

88 DeLorme, M., Datla, R., 2007)):

89 What is specific to boats is that the frontal surface depends on the speed. In fact, when the boat accelerates,
90 the water dynamic lift increases and the boat trim and draught change. If it is considered as having a rectangular
91 parallelepipedic hull, a rectangular parallelepipedic wheelhouse and a bridge parallel to the keel³, the frontal
92 surface of the boat S_{boat} is :

93 $S_{boat} = S_{hull} + S_{house}$

94 With : $S_{house} = B_{SS} (H_{SS} - DBH \tan(\tau))$

95 $S_{hull} = B_{max} (LOA \tan(\tau) + H_{hull} - D)$

96 So $D_{aero} = \frac{1}{2} \rho_{air} S_{boat} C_x v^2$

³ If the bridge forms an angle τ_1 with the keel, the angle τ in the S_{house} calculation must be replace by $\tau_1 + \tau$. τ_1 is positive when in opposite direction of vector g .

97 To inject this force in the equation of the pitching moment, $C_{p_{aero}}$ need to be determined. As the expression of
 98 D_{aero} shows it, the aerodynamic drag is proportional to the frontal surface of the boat. The aerodynamic drag can
 99 be divided into the “wheelhouse aerodynamic drag” and the “hull aerodynamic drag”. $C_{p_{aero}}$ is equal to VCG less
 100 the vertical coordinate of the barycenter of both hull and house aerodynamic center of pressure.

101
$$C_{p_{aero}} = VCG - \frac{0.5 \text{ Shouse (Hss} - \text{DBH Tan}(\tau)) + 0.5 \text{ Scoque (Zh} + \text{DBH Tan}(\tau))}{\text{Shouse} + \text{Scoque}}$$

Hull	Length of Waterline	L _{WL}	13,92	m
	Beam (at waterline)	B	3,50	m
	VCG	VCG	1,31	m
	Displacement	Δ	24276	kg
	Deadrise @ Transom	β _T	19,00	°
	Deadrise @ Amidships	β _x	23,00	°
	Angle of Thrust Line	ε	0,00	°
	LCG	f	0,63	m

Step	Step 1	number of steps	nb	0	
		Distance from Transom to step 1	d1	2,50	m
	angle du step1 par rapport à l'horizon	τ2	2,00	°	
	Deadrise before step 1	β 1	11,00	°	
	First step height	H1	0,05	m	
	beam at step 1 (at waterline)	B1	2,00	m	
	angle between the keel in front, and keel behind step1	φ1	0,00	°	
	Step 2	Distance from Transom to step 2	d2	4,00	m
		angle du step2 par rapport à l'horizon	τ2	3,00	°
		Deadrise before step 2	β 2	24,00	°
second step height		H2	0,20	m	
beam at step 2 (at waterline)		B2	3,00	m	
angle between the keel in front, and keel behind step2	φ2	1,00	°		

aero	Length Overall	LOA	15,38	m
	Maximum Beam	B _{max}	3,60	m
	Moulded Depth of Hull	Z	2,15	m
	Height of House	H _{SS}	1,84	m
Breadth of House	B _{SS}	2,31	m	
distance between bow and house	DBH	4,20	m	
aero drag coefficient	C _x	0,80		

Site	water	temperature	Tw	18,00	°C
		salinity	Sal	35,00	g.L-1
	air	temperature	Ta	20,00	°C
global		g_SI	9,81	m/s ²	

Engine + propulsion	Propulsion type	
	Engines	
	Rated Power	1192 kW
	number of engines	2
	Fuel Capacity	3500 L
mecanical losses	5 %	

Optimisation	initial displacement	5 000	kg
	step	200	kg
	inialial LCG	2,0	m
	step	0,10	m

speed	V (studied speed)
	[kn]
	5
	6
	7
	8
	9
10	
11	
12	

Figure 1 : PPT tool's inputs

104 Once $C_{p_{aero}}$ is known, the equation 35 of Savitsky (**Savitsky, 1964**) can be modified to become :

105
$$M = mg \left[\frac{c}{\cos(\tau)} (1 - \sin(\tau) \sin((\tau + \epsilon)) - f \sin(\tau)) \right] + Df(a - f) + Dair C_{p_{aero}}$$

106 Data in step section are used to compute “Savitsky's Method used behind the Step” developed by Svahn in
 107 (**Svahn, 2009**). For this paper the number of step will remain 0 as the studied boat is a classical hard chine
 108 monohull boat.

109 Data in site section are used to compute water viscosity and density, air density and to give a classical
 110 engine de-rating.

111 The engine + propulsion section permits:

- 112 -to select a propulsion type (classical propeller, surface propeller, hydrojet ...) to calculate its OPC.
- 113 -to select an engine to compute the fuel consumption
- 114 -to take into account the mechanical losses.

115 The engine consumption calculation will not be detailed in this paper because the focus is made only on
 116 power prediction. The hydrojet OPC calculation will be detailed as the studied boat is equipped with two of
 117 them and as it directly influences the power prediction.

118 To calculate the OPC of a given jet, the thrust prediction curve, **Figure 3**, must be given by the manufacturer.
 119 Each black curve on this graph gives the jet thrust versus boat speed, for a given power. The green dotted curve
 120 represents the limit of the cavitation zone.

121 To use it automatically in a computer procedure the OPC coefficients need to be determined for each speed
 122 step:

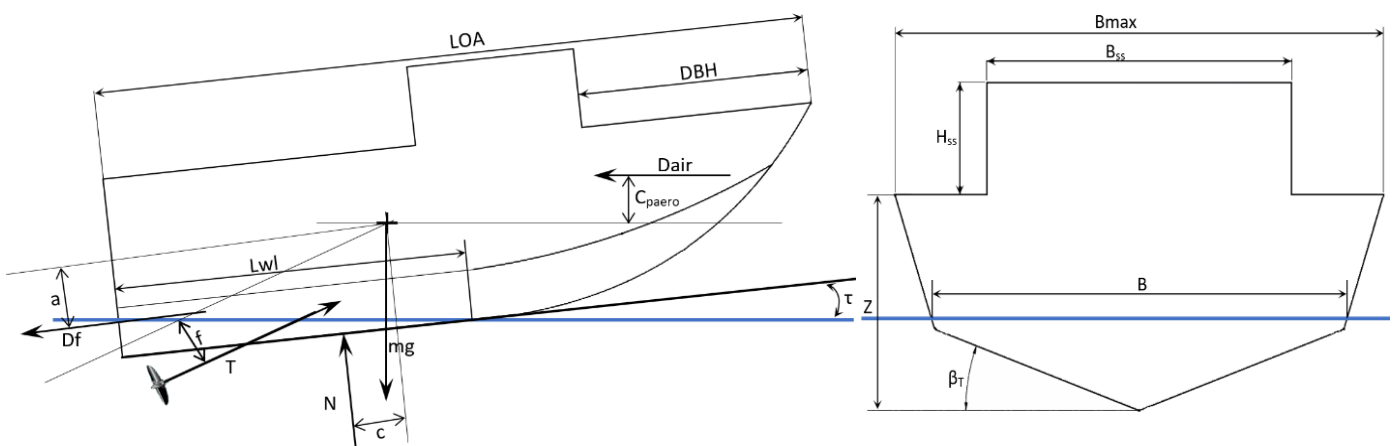
$$123 \quad OPC = \frac{T \cdot v}{P_{jet}}$$

124 This relation transforms the thrust versus speed, for a given power, curves into the OPC versus speed, for a
 125 given power, curves. Then comparing the required thrust with all that are shown on the different curves allows to
 126 select the best value between all the possible (a graph as the one on **Figure 3** will give ten possible values of OPC
 127 for each speed step). The more iso-power curve available the more precise this method will be.

128 The fuel capacity permits to calculate the boat operating range and endurance.

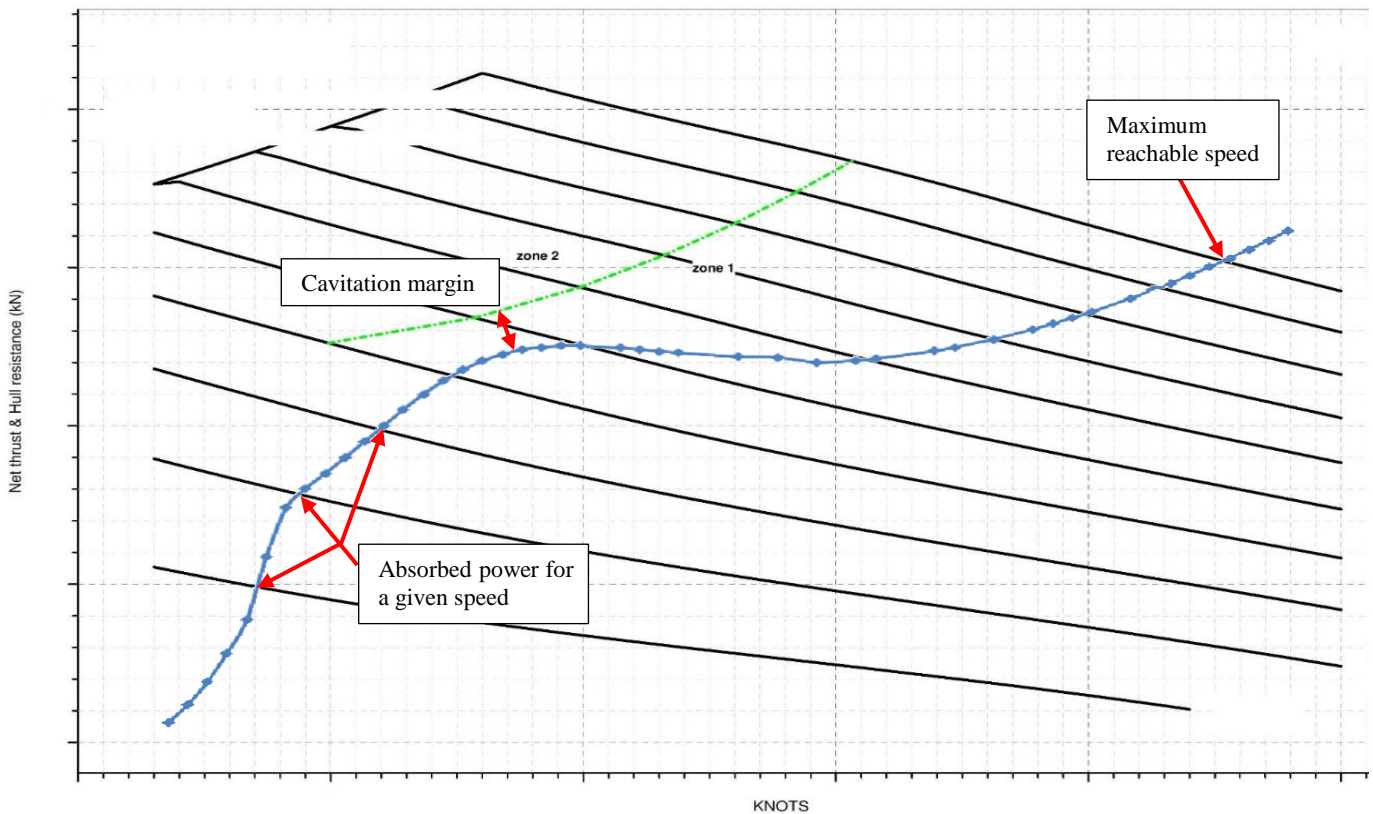
129 The last item of this section, mechanical losses, allows to compute $OPC' = OPC * \eta_{méca}^4$ which eventually
 130 leads to the calculation of the real required power for a given speed :

$$131 \quad P_{calculated} = \frac{v \cdot R_t}{OPC'}$$



132 **Figure 2 : boat outlines with its main inputs and acting forces**
 133

⁴ For the rest of the study $\eta_{méca}$ will be equal to 95%



1
135

Figure 3 : Typical thrust prediction of a jet manufacturer

136 The optimization section is used to simulate 11 cases in which the boat weight or the center of gravity slightly
 137 differs. This add-on helps to target the best compromise zone in terms of weight and center of gravity's
 138 longitudinal position during the early stages of a preliminary-study.

139 The speed section permits to enter speeds of interest. The more speeds the longer the total calculation will
 140 be.

141 This rapid overlook of the PPT helps to understand how calculations are made. The next section will present
 142 the boat's data used to make the comparison.

143 VI. BOAT AND USEFUL DATA

144 The boat used to compare the PPT with real measurements is the Plascoa 1650, **Figure 4**. It is produced in
 145 series at CNC Couach. More than 50 have been produced. These military vessels are built on a planing hull to
 146 intercept other boats at speeds over 55 knots. The line plan is confidential so it will not be presented in this paper.
 147 However data required for simulation are available on Figure 5, Figure 6 and in appendix 1 : PPT inputs variation
 148 range.

149 A sample of 35 ships have been chosen to be compared with the PPT prediction. They have been tested in real
150 conditions in the Arcachon Bay, over a period of 11 month. This long time range permits to cover a panel of
151 different weather conditions.



152
153

Figure 4 : rendering of the 1650 Plascoa

154 The required data had been classified as being of two types:

155 -General data, which are constant from boat to boat, (**Figure 5**).

156 -Specific data, which are boat dependent, (**Figure 6**).

157 VCG is considered as being constant because it can only vary from few centimeters, which has a very small
158 impact on power performances, and it is very difficult to measure⁵.

159 Site data (air temperature, water temperature and salinity) had been approximated with average values.

160 For each of the 35 studied boats sea trials reports have been made. They are used to validate the performance
161 of the propulsion line in real conditions.

162 Data are collected every 200 engine rpm. Those which are of interest for this study are the absorbed engine
163 power and the corresponding boat speed.

164 All the 35 boats are equipped with interceptors which are used to reduce drag at low speed. The impact of
165 this system will not be studied in this paper because for the considered tests the interceptors were not deployed.

166 If one is interested in implementing interceptors in a prediction code (Ekman et al, 2016) present two methods
167 of doing so.

⁵ Reference : Bureau Veritas : Rules for the classification and the certification of Yachts ; Part B : Hull and Stability ; Chapter 3 Stability ; Appendix 1 : Inclining Experiment and weighing test.

Hull	Vertical position of the center of gravity (origin at boat transom)		VCG	1,31	m
	Deadrise angle at Transom		β_T	19,00	°
	Deadrise angle at mid ships		β_x	23,00	°
	Inclination of thrust line relative to keel line		ε	0,00	°
	Distance between T and CG measured normal to T		f	0,63	m
Hull aero	Length Overall		LOA	15,38	m
	Maximum Beam		B_{max}	3,60	m
	Moulded Depth of Hull		Z	2,15	m
	Height of House		H_{SS}	1,84	m
	Breadth of House		B_{SS}	2,31	m
	distance between bow and house		DBH	4,20	m
aero drag coefficient		Cx	0,80		
Site	water	temperature	Tw	18,00	°C
		salinity	Sal	35,00	g.L-1
	air	temperature	Ta	20,00	°C
		global	g_Sl	9,81	m/s ²
Engine + propulsion	Propulsion type		Kamewa A3 40		
	Engines				
	Rated Power	1192	kW		
	number of engines	2			
	Fuel Capacity	3500	L		
	mecanical losses	5	%		

168
169

Figure 5 : General data of the Plascoa 1650

Hull	Length of Waterline		L_{WL}	13,92	m
	Beam (at waterline)		B	3,50	m
	Displacement		Δ	24276	kg
	Longitudinal position of the center of gravity (origin at boat transom)			5,35	m

170
171

Figure 6 : Example of specific data of the Plascoa 1650

172

VII. MFACTOR IMPACTS ANALYSIS

173

As it is explained in the PPT description, the tool first calculates the boat drag with the Savitsky procedure and

174

then corrects this drag with the Mfactor coefficient of (Blount, Fox, 1976).

175

$$\text{With Mfactor} = 0.98 + 2\left(\frac{LCG}{Bpx}\right)^{1.45} e^{-2(Fv - 0.85)} - 3\left(\frac{LCG}{Bpx}\right) e^{-3(Fv - 0.85)}$$

176

According to the authors, this coefficient can be used while:

177

$$Fv \geq 1,0$$

178

$$\frac{LCG}{Lp} \leq 0,46$$

179

For the 1650 Plascoa $Lp = 14.7m$

180

And on the 35 studied boat $LCG \leq 5,45m$

181

$$\text{So } \frac{LCG}{Lp} \leq 0,371 \leq 0,46$$

182

For this boat $Fv \geq 1$ when the speed is over 11 knots.

183 To further enhance the precision of the PPT, a better understanding of how this Mfactor impacts the
184 calculation is required. So numerical tests have been conducted with and without this coefficient.

185

186 **VII.1. CALCULATION WITHOUT MFACTOR**

187 The first study was to overlap the absorbed power versus boat speed for both theoretical data (blue curve)
188 and experimental data (red curve), see **Figure 7**.

189 In order to refine the study, the difference between theoretical and real points have been computed. In order
190 for it to be representative it has been divided by the maximal engine power (here 1192 kW).

191 So

$$192 \quad E = \frac{P_{measured} - P_{computed}}{P_{max}}$$

193 If this difference is positive, the PPT underestimate the required power, if negative then it overestimate the
194 required power.

195 The 361 points have been reported on **Figure 8**.

196 Extreme values (rounded in blue on **Figure 8**) belong to three different boats and represent 6 values over
197 361 (1.66%). Additionally, these three boats are the first three to have been studied. So it can be considered as
198 being not representative of the series.

199 According to **Figure 7** and **Figure 8** it is noticeable that the PPT is oversizing the required engine power
200 for speeds under 9 knots and to a slightly lesser extent in the interval [14;24] knots. The local average of the
201 differences is respectively -5.12% and -1.92% while the overall average is -0.35%.

202 However the PPT is underestimating the required power for speed over 58 knots, the average excluding the
203 first three boats is 3.63%.

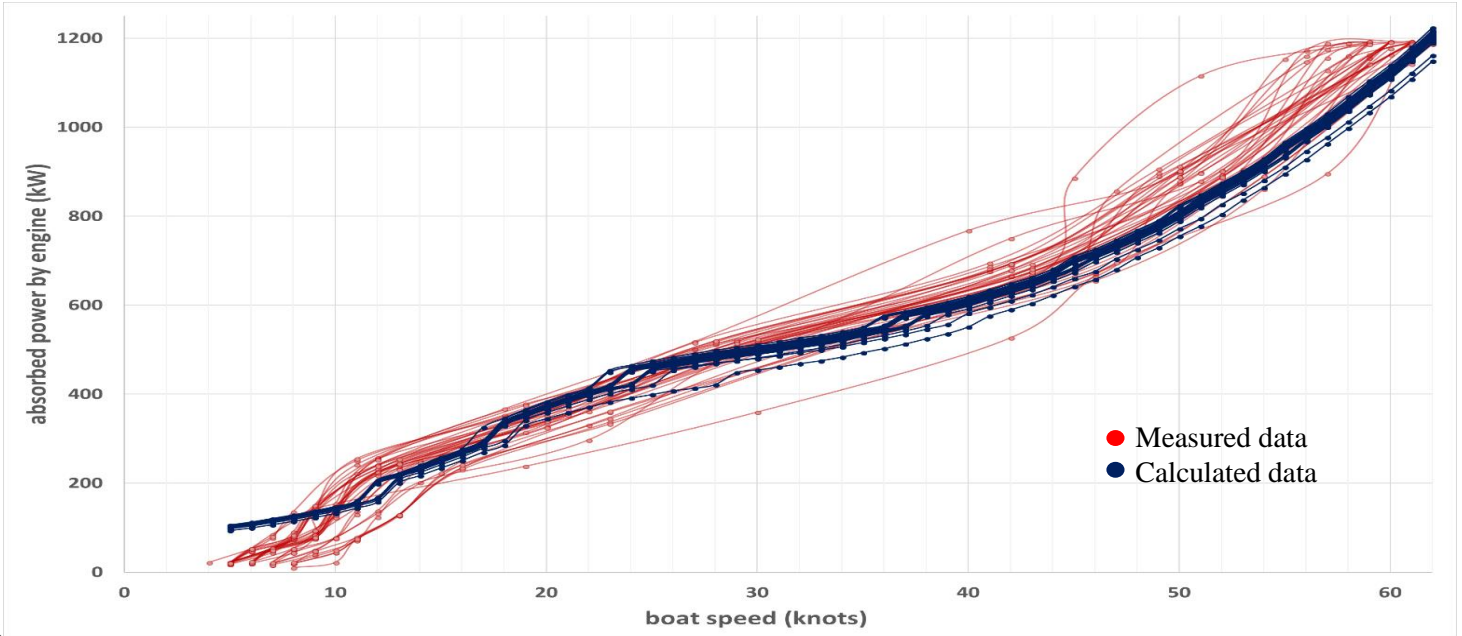
204 In order to better understand the differences' repartition an histogram is shown on **Figure 9**. It allows to sort
205 values within an interval of [-20% ; 20%] with a step of 2%. Violet corresponds to the number of values while
206 blue gives the percentage of the number of values regarding the total number of values.

207 According to this histogram all the differences are included in the interval [-11.83% ; 24.87%].

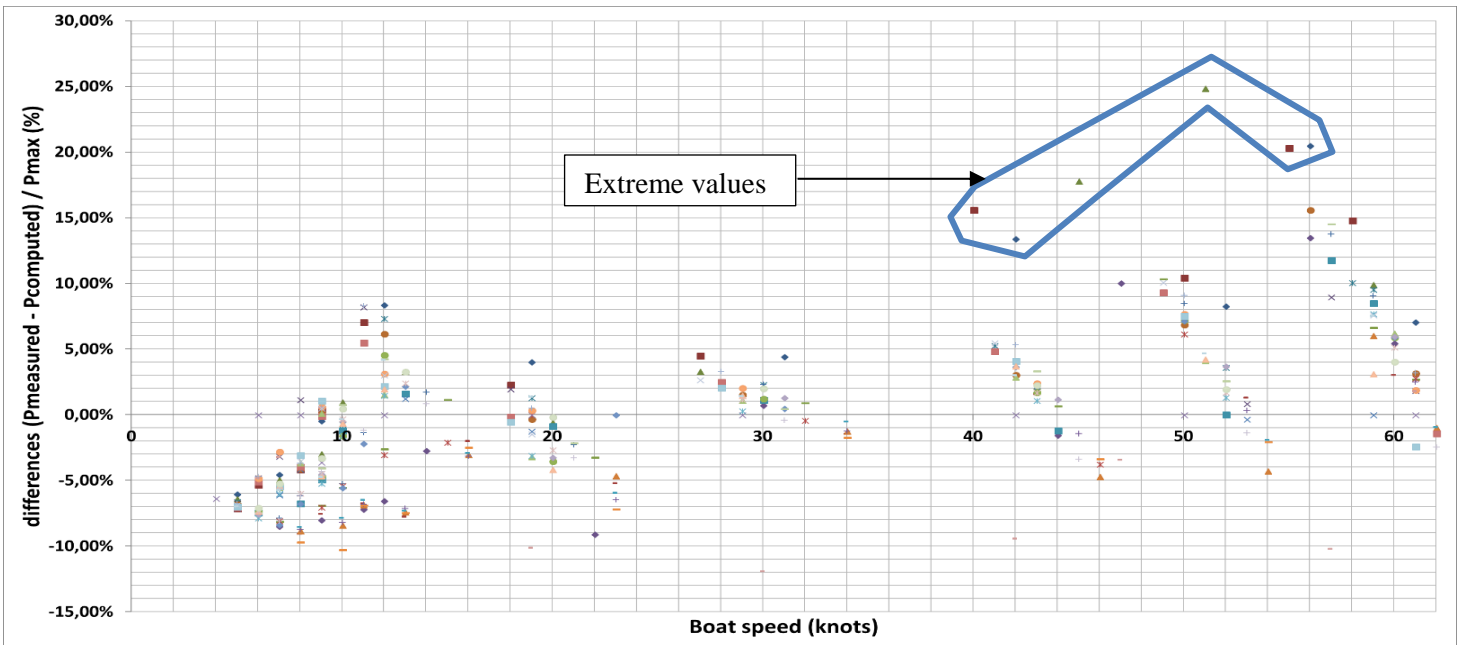
208 Values are mostly negatives and dispersed in the interval [-8% ; 6%].

209 Indeed :

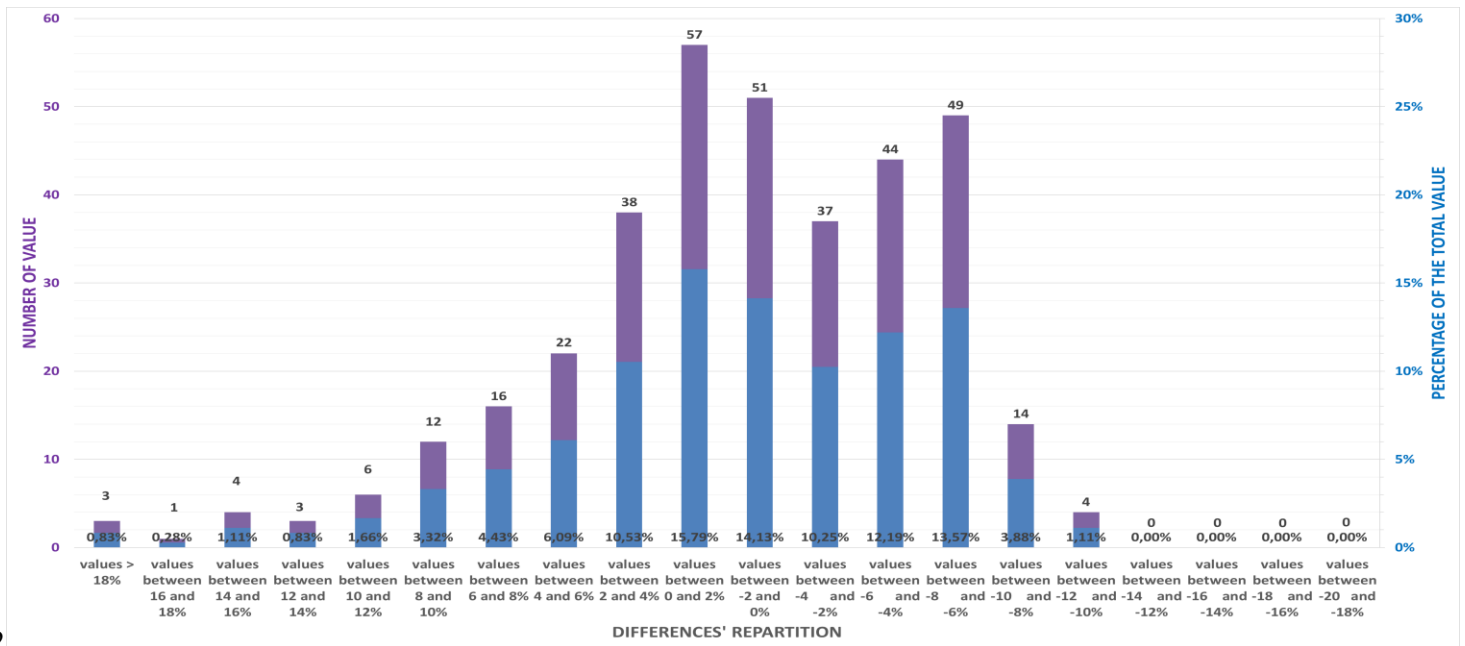
- 210 • 55,12% of the total values are negatives.
- 211 • 29,92% are included in [-2% ; 2%].
- 212 • 50,69% are included in [-4% ; 4%].
- 213 • 94,18% are included in [-10% ; 10%].



215 → Figure 7 : Overlapping of theoretical and experimental curves



217 → Figure 8 : Power difference versus boat speed



→ Figure 9 : Differences' repartition

VII.2. CALCULATION WITH MFACTOR

This study follows the same presentation as the previous one.

According to **Figure 10**, the oversizing between 14 and 24 knots is more pronounced than if the Mfactor is not used. Additionally the required engine power is underestimated for speeds under 8 knots and values are even negatives for speeds under 7 knots. This observation confirms the model's limits given by the authors.

As in previous parts, graphic of **Figure 11** permits to be more precise:

All the differences are included in the interval [-13.89%;30.86].

The average of the differences for speeds under 9 knots is 7.32% and for the interval [14;24] knots it is -5.72%.

The average for speed over 58 knots excluding the first three boats is 5.59%.

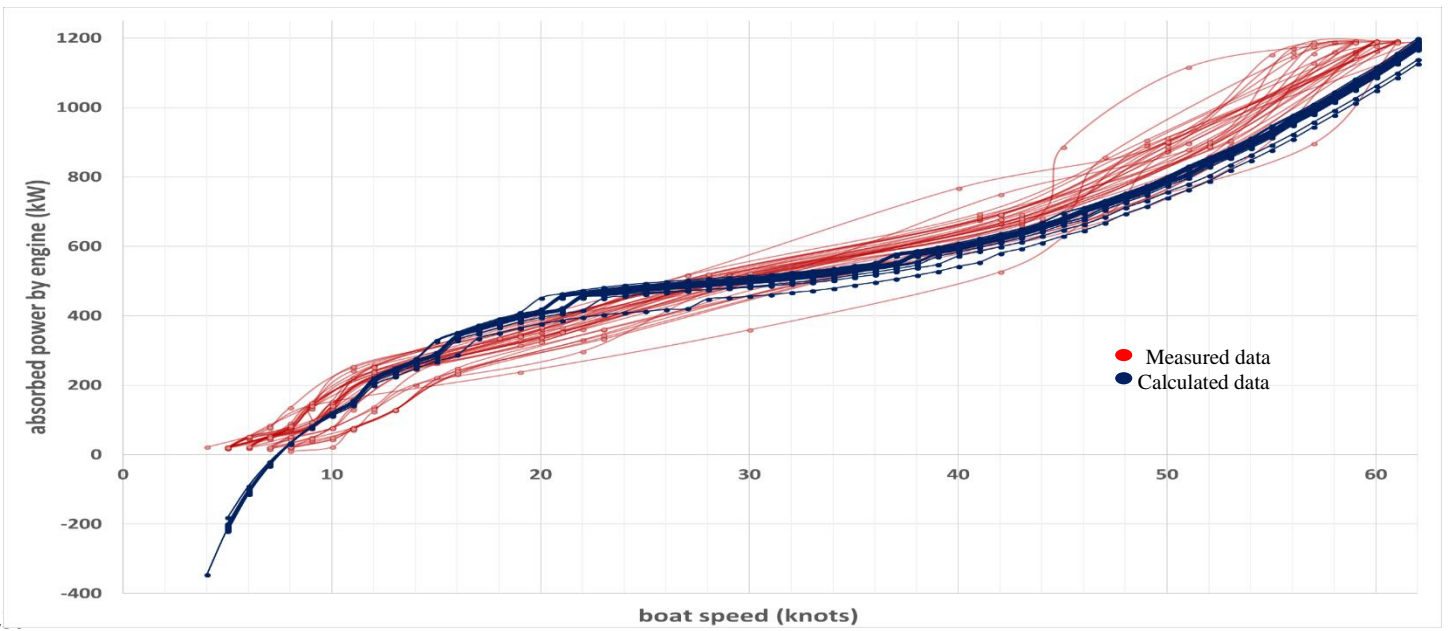
The overall average difference is 3.14%.

Comparing to Savitsky's theory alone, the histogram on **Figure 12** reveals that a higher number of values are over 18% of difference. This is due to the fact that in addition to the first three boats values, values for speeds under 8 knots increase this statistic.

The histogram also highlights that values are more dispersed compared with Savitsky theory alone. Indeed :

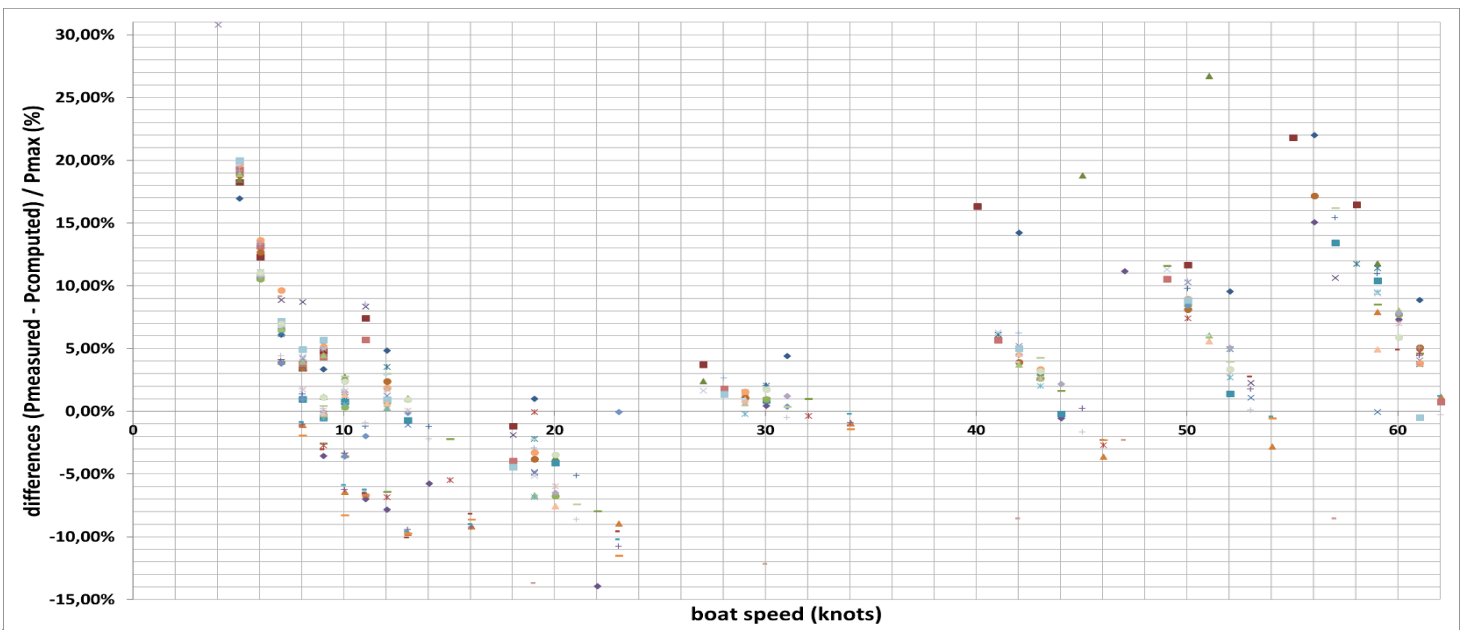
- 31,3% of the total values are negatives.
- 28,25% are included in [-2% ; 2%].
- 46,54% are included in [-4 ; 4%].

238 • 82,55% are included in [-10 ; 10%].



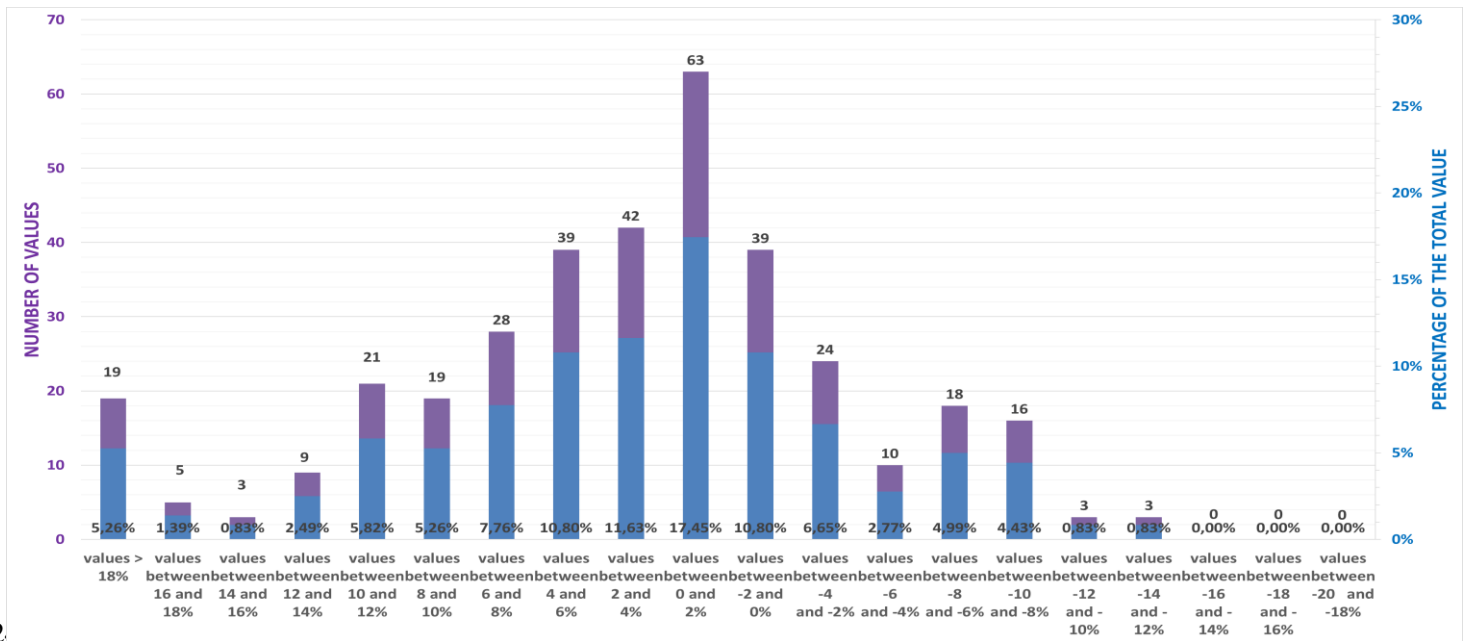
240

Figure 10 : Overlapping of theoretical and experimental curves



242

Figure 11 : Power difference versus boat speed



244 Figure 12 : Differences' repartition tool's optimisation

245 VIII. TOOL'S OPTIMISATION

246 Taking into account observations that have been made in the **VII Mfactor impacts analysis** part, the PPT had
 247 been modified to minimize differences between measurements and predictions.

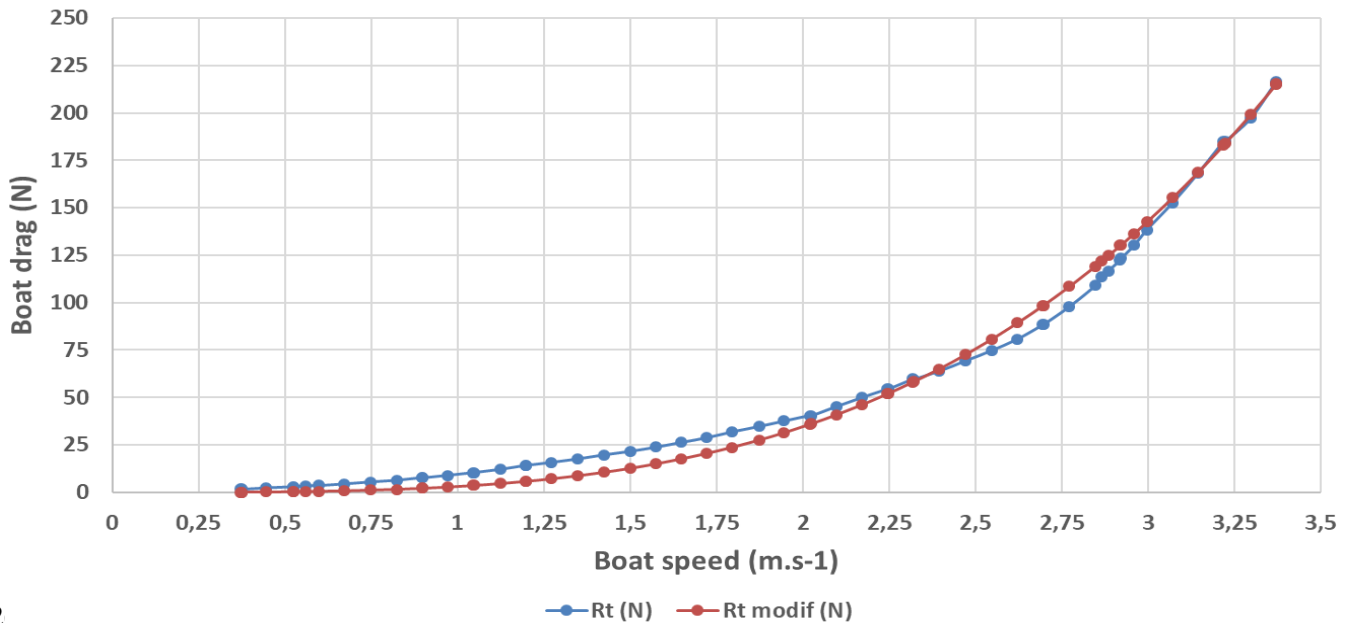
248 The purpose of these modifications is to minimize changes made on Savitsky's theory and to keep a physical
 249 meaning. In this new version, the Mfactor had been suppressed. The average of -1.92% between 14 and 24 knots
 250 is considered acceptable because smaller than 2% in absolute value.

252 VIII.1. CORRECTION FOR LOW SPEED

253 The paragraph **VII.1 Calculation without Mfactor** highlights a lack of precision of the Savitsky
 254 procedure for speed below $C_v = 0.9$. In order to reduce it a new correction has been employed. To keep it
 255 very simple, a model under the form $R_{tv} = k \times V^b$ with k constant is studied.

256 When the C_v is below 0.9 the considered boat is in displacement mode. During this phase the drag
 257 versus speed of the boat seems to follow a polynomial curve (**VII.1 Calculation without Mfactor, (Sunny**
 258 **Verma., Shiju John, 2010), (Olivieri et al, 2001)**). The Figure 13 below illustrates this observation. The
 259 R_t curve gives the experimental drag measured for the Insean 2340 (**Olivieri et al, 2001**) and the R_t modif
 260 curve is plotted according to the relation:

261 $R_{tv} = \frac{R_{tmax}}{V_{max}^{3.5}} \times V^{3.5}$ with R_{tv} the drag calculated at the speed V , R_{tmax} the maximum measured
 262 drag measured at V_{max} the maximum speed reached during the test (3.371 m.s^{-1}).



264 Figure 13 : comparison between a polynomial curve and the real drag of the Insean 2340 Model.

265 After reading the paper from (Sunny Verma., Shiju John, 2010) it comes that the 1650 Plascoa is not
 266 the only planning boat where the drag predicted by Savitsky procedure is equal to the measured drag for
 267 C_v approximatively equal to 0.9 (~ 10.25 knots for the 1650 Plascoa). According to this observation, two
 268 values of this curve are known. The boat drag at 0 knot is obviously equal to 0 and at $C_v = 0.9$ it is almost
 269 equal to the drag calculated with the Savitsky procedure.

270 Let $R_{t0.9}$, R_{tv} and $V_{0.9}$ respectively the drag computed at $C_v = 0.9$ with Savitsky's theory, the drag computed
 271 at the speed V and $V_{0.9}$ the speed at $C_v = 0.9$.

272 As the drag at $C_v = 0.9$ is known, $k = \frac{R_{t0.9}}{V_{0.9}^{3.5}}$. The real difficulty is to determine b . As the authors did not know
 273 all the different coefficients from the 4 boats studied by (Sunny Verma., Shiju John, 2010) the curves they
 274 produced have been reused to conduct an empirical study to find the best b possible. The results are presented
 275 below. For each of the four boats, 3 different b have been tested.

276 On each graph are plotted:

277 -The measured drag : R (N)

278 -The calculated drag by the correction formula $R_{tv} = \frac{R_{t0.9}}{V^{0.9^b}} \times V^b$: Rmodif (N)

279 -The calculated drag with the Savitsky procedure : Rsavit (N)

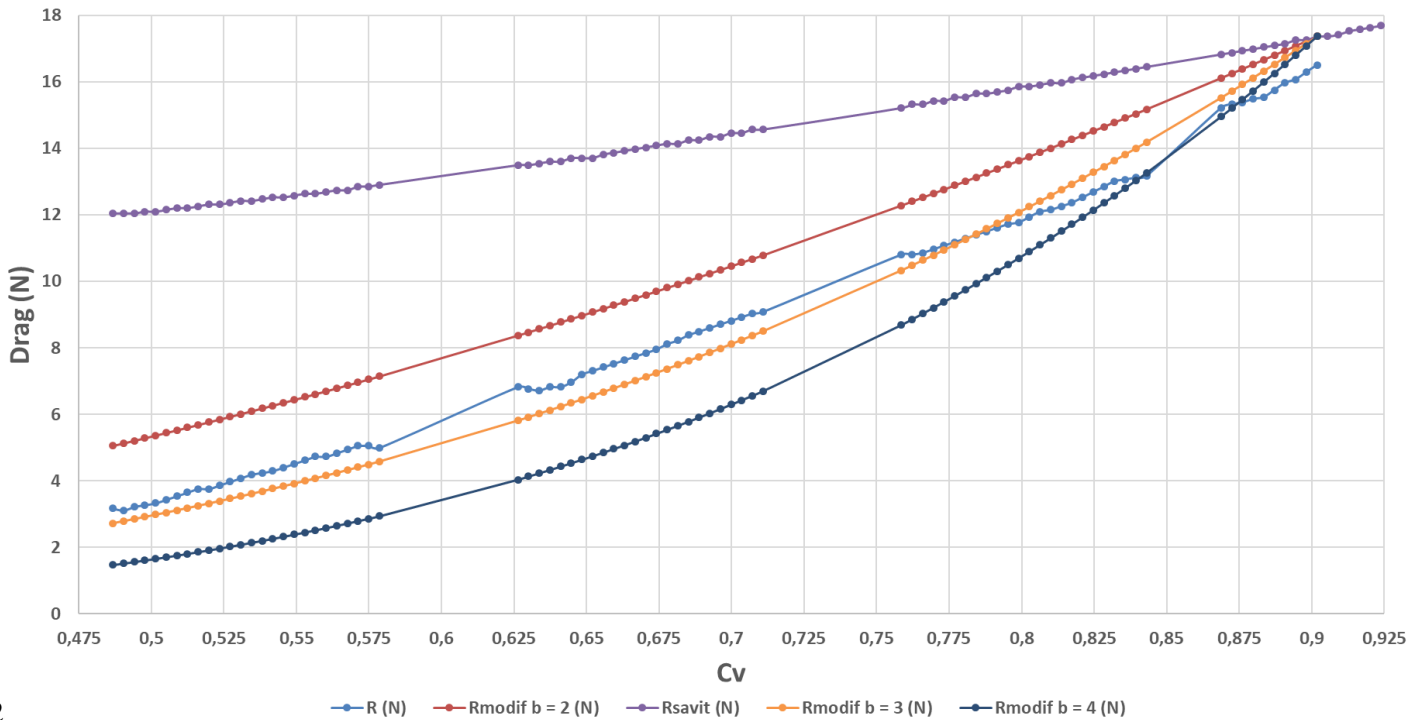
280 For each tested b are calculated:

281 -The difference = $\frac{R(N) - R_{modif}(N)}{R(N)}$: difference (%)

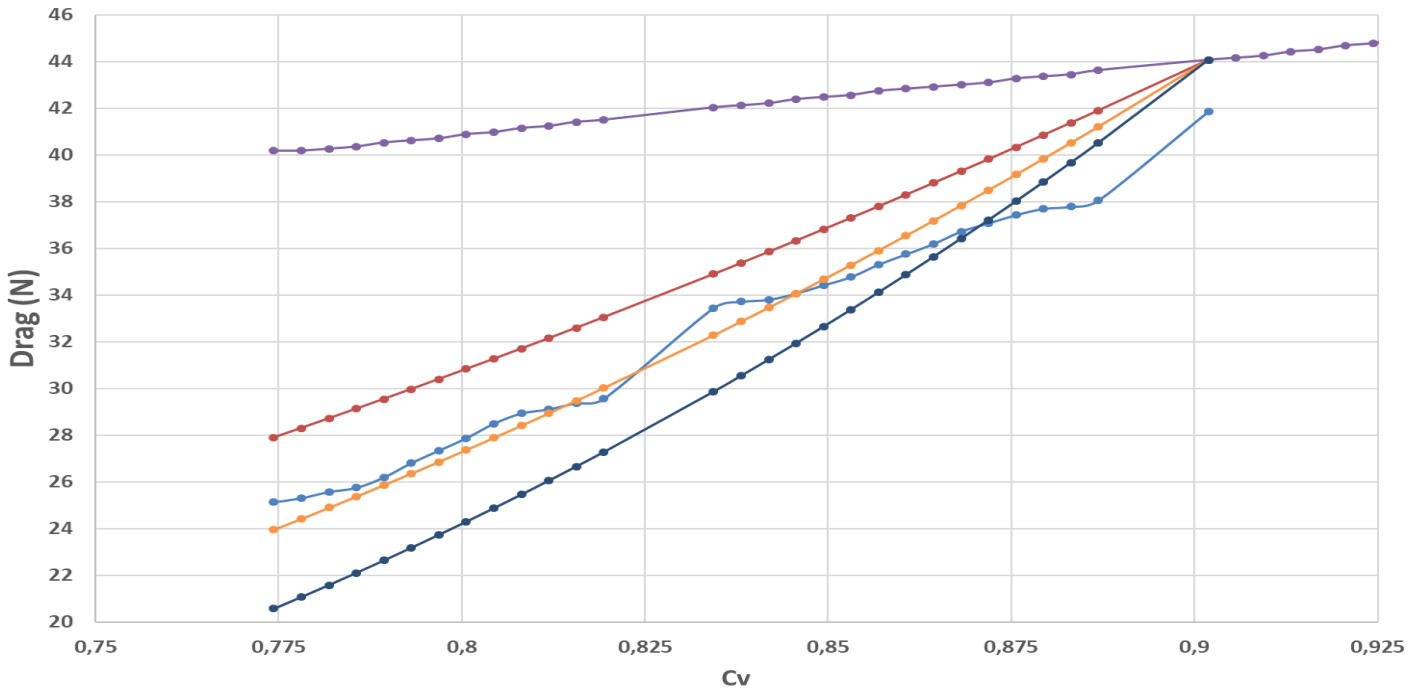
282 -The corrected difference = $\frac{R(N) - R_{modif}(N)}{R_{0.9}(N)}$ with $R_{0.9}(N)$ the measured drag at $C_v = 0.9$:

283 corrected difference (%)

284 The Figure 18 is summing up the maximum, the minimum and the average of these two calculation for
 285 all the tested b.

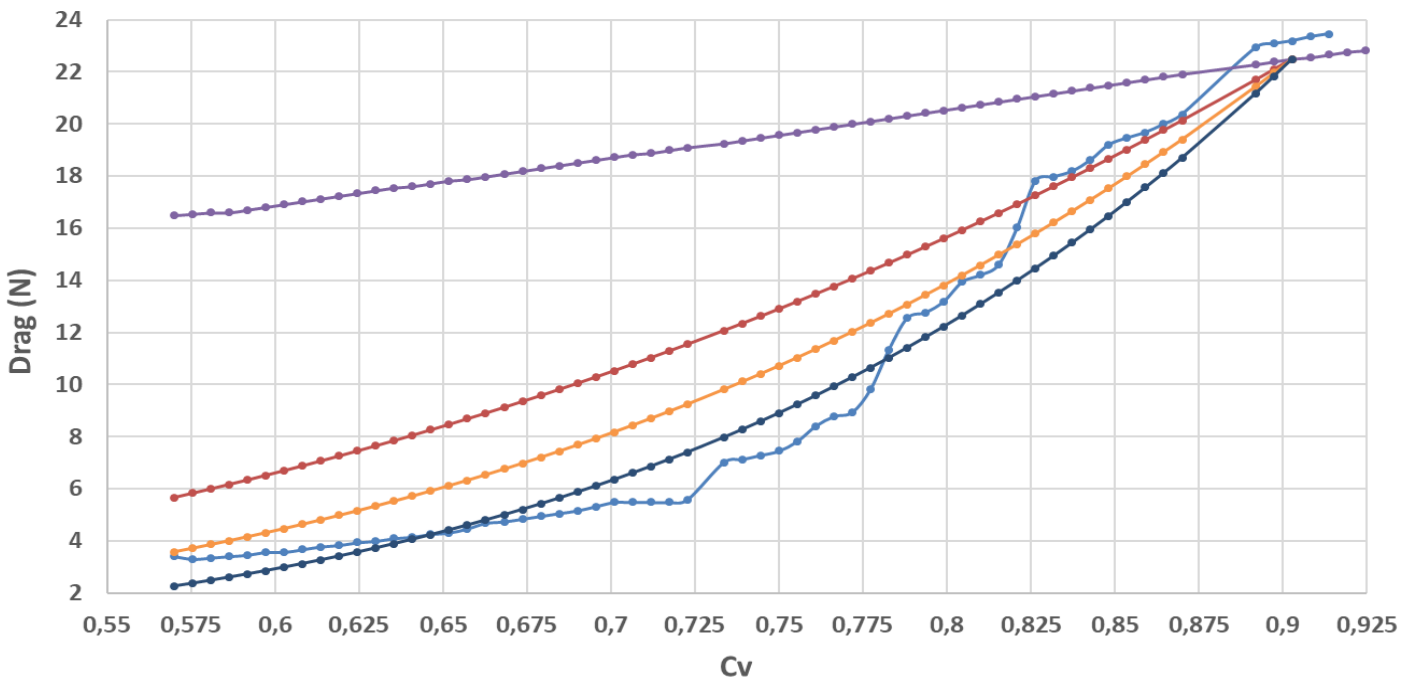


287 **Figure 14 : b = 2, 3 and 4 for vessel number 1 (refer table 7 (Sunny Verma., Shiju John, 2010))**



2
289

Figure 15 : b = 3, 4 and 5 for vessel number 2 (refer table 7 (Sunny Verma., Shiju John, 2010))



2
291

Figure 16 : b = 3, 4 and 5 for vessel number 3 (refer table 7 (Sunny Verma., Shiju John, 2010))

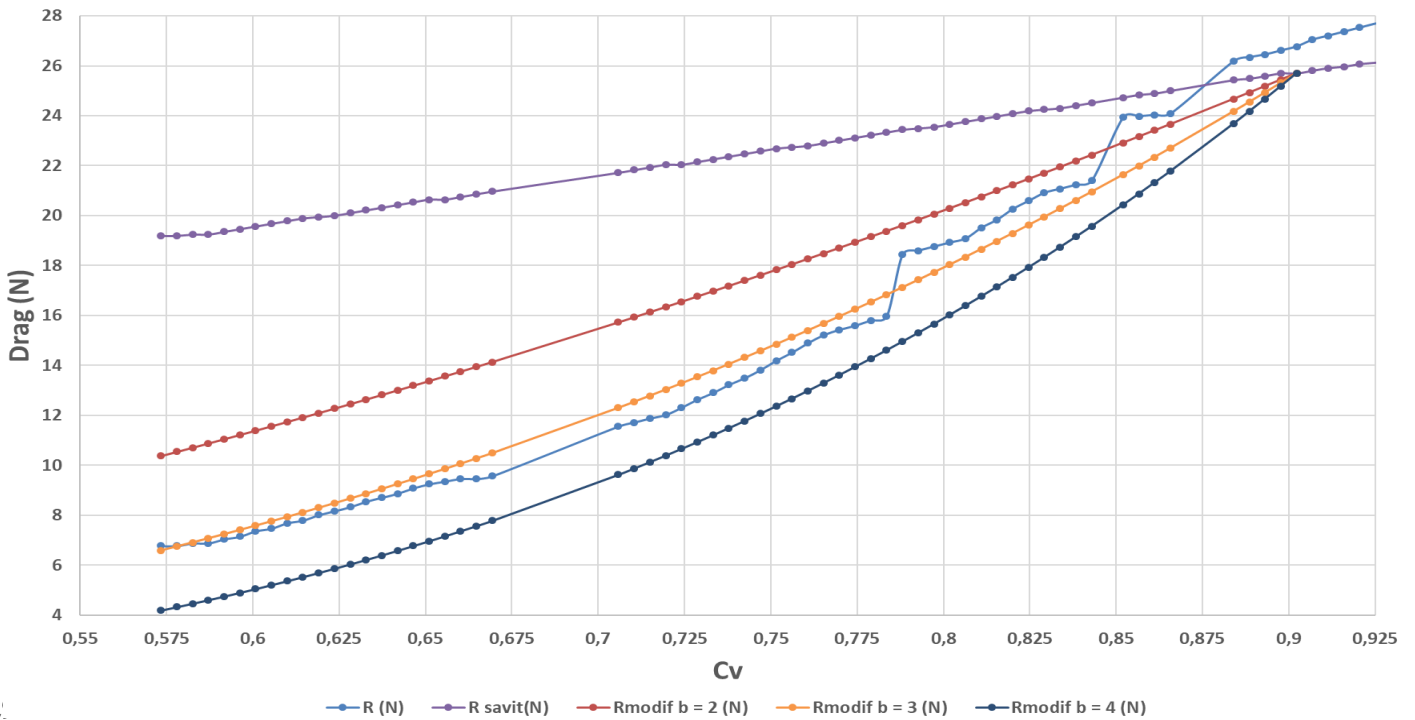


Figure 17 : b = 2, 3 and 4 for vessel number 5 (refer table 7 (Sunny Verma., Shiju John, 2010))

		vessel 1			vessel 2			vessel 3			vessel 5		
		b = 2	b = 3	b = 4	b = 3	b = 4	b = 5	b = 3	b = 4	b = 5	b = 2	b = 3	b = 4
difference	Minimum	-64.7%	-7.7%	-5.2%	-13.1%	-8.3%	-6.5%	106.7%	-65.5%	-32.5%	-58.1%	-9.6%	9.5%
	Maximum	-5.2%	14.8%	53.5%	-4.3%	4.7%	18.2%	5.4%	11.3%	33.7%	16.2%	22.6%	38.1%
	Average	-26.5%	5.4%	26.6%	-9.0%	-0.6%	6.9%	-57.1%	-23.3%	1.7%	-16.7%	7.7%	25.7%
corrected difference	Minimum	-13%	-6.1%	-5.2%	-8.3%	-2.6%	-1.7%	-25.7%	-15.8%	-7.8%	-15.6%	-3.1%	6.1%
	Maximum	-5.2%	6.1%	16.9%	2.4%	4.8%	10.9%	5.3%	8.7%	14.5%	13.1%	18.2%	23%
	Average	-10.5%	1.2%	9.6%	-4.5%	1.4%	6.7%	-12.9%	-4.7%	1.7%	-3.3%	5.9%	12.9%

Figure 18 : table summing up the differences

According to all these curves a general trend is highlighted. Increasing b causes the Rmodif curve to bend and be on a longer range under the real drag curve R, so the real drag is more under predicted. For all the four boats, the value of b which minimize the difference, between the two curves R and Rmodif, without too much under prediction is always between 2 and 4.

Indeed : -for vessel number 1, $2 < b < 3$

-for vessel number 2, $b \sim 4$

-for vessel number 3, $b \sim 4$

-for vessel number 5, $2 < b < 3$

304 To conclude this study on the empirical formula $R_{tv} = \frac{R_{t0.9}}{V_{0.9}^b} \times V^b$, on a first approach taking $b = 3$ is a
305 good compromise. The risk of under prediction is low and the drag prediction precision is noticeably
306 increased compared with the classical Savitsky procedure.

307

308 **VIII.2. Cx MODIFICATION**

309 To correct the differences observed for speeds over 58 knots only the C_x was increased. After few iterations
310 1.1 is the value which gives the best correlation with tests. As a reminder the C_x value for a plane plate is equal
311 to 1 and for a car it is often between 0.3 and 0.4.

312 Such a high value for the 1650 Plascoa can be explained by two factors:

- 313 • The boat shape is not aerodynamic enough.
- 314 • Mast, antennas, radars ... are not taking into account to compute the frontal surface
315 of the ship. So it artificially increases the vessel C_x .

316

317 **VIII.3. RESULTS**

318 According to **Figure 19** and **Figure 20** the power sizing for low speed is much more precise. The average
319 of the differences for speed under 9 knots is 0.24% while it was -5.12% with Savitsky theory alone.

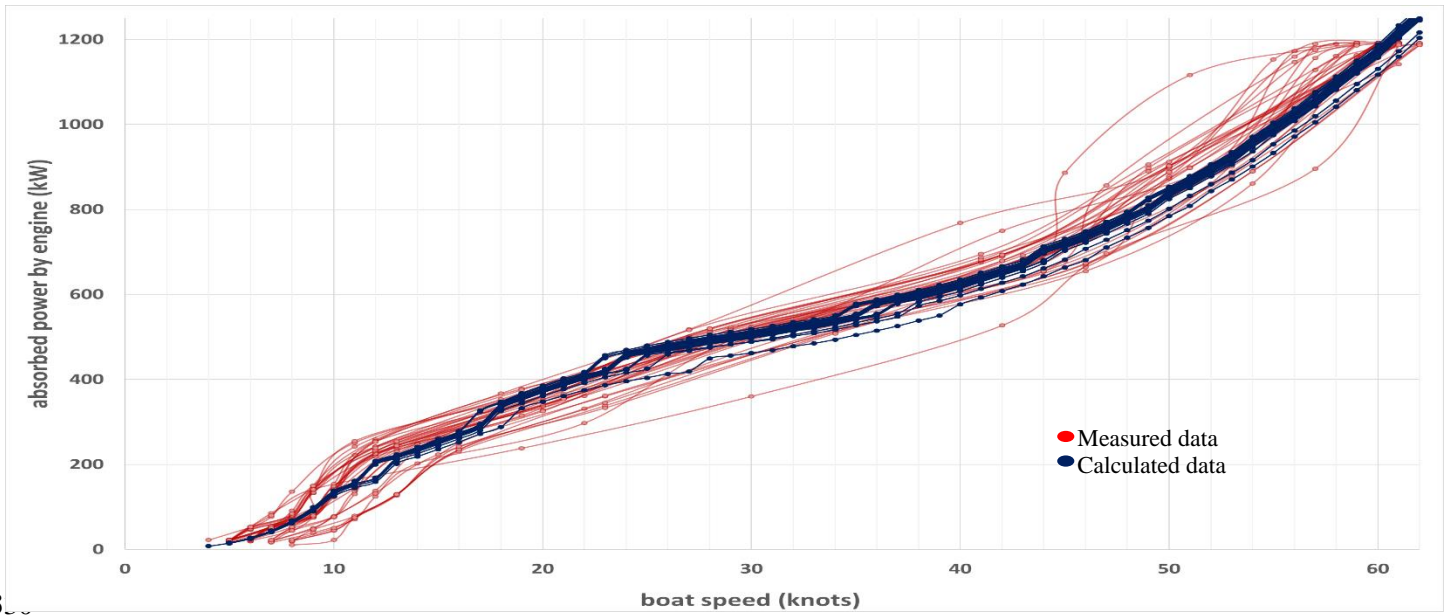
320 The oversizing in the interval [14;24] knots is increased because of the C_x increase, the local average being
321 -2.12% while it was -1.92% with a C_x of 0.8.

322 The average for speeds over 58 knots excluding the first three boats is -0.31% while it was 3.63% with a
323 C_x of 0.8.

324 All the differences are included in [-13.63%; 22.3%]. The overall average is 0.203%.

325 The histogram **Figure 21** shows a values' distribution more centered around zero than with previous tests:

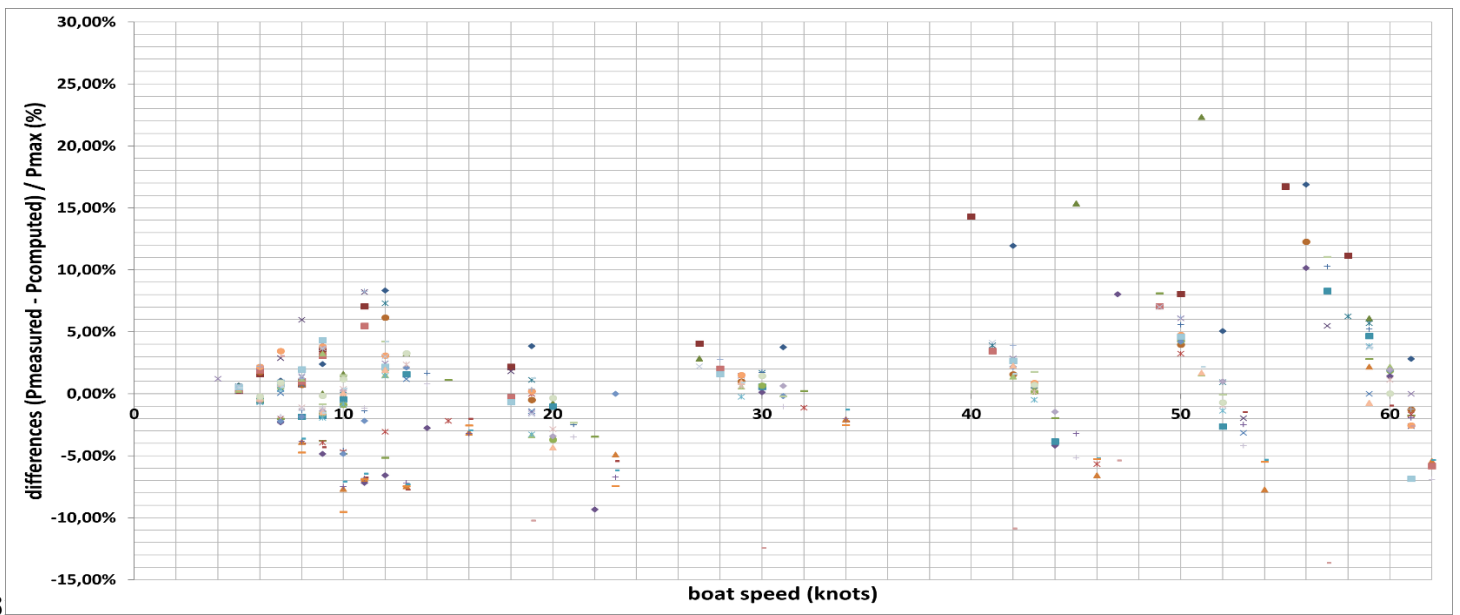
- 326 • 44,60% of the values are negatives.
- 327 • 48,2% are included in [-2% ; 2%].
- 328 • 72,58% are included in [-4% ; 4%].
- 329 • 95,84% are included in [-10% ; 10%].



331

Figure 19 : Overlapping of theoretical and experimental curves

332



334

Figure 20 : Power difference versus boat speed

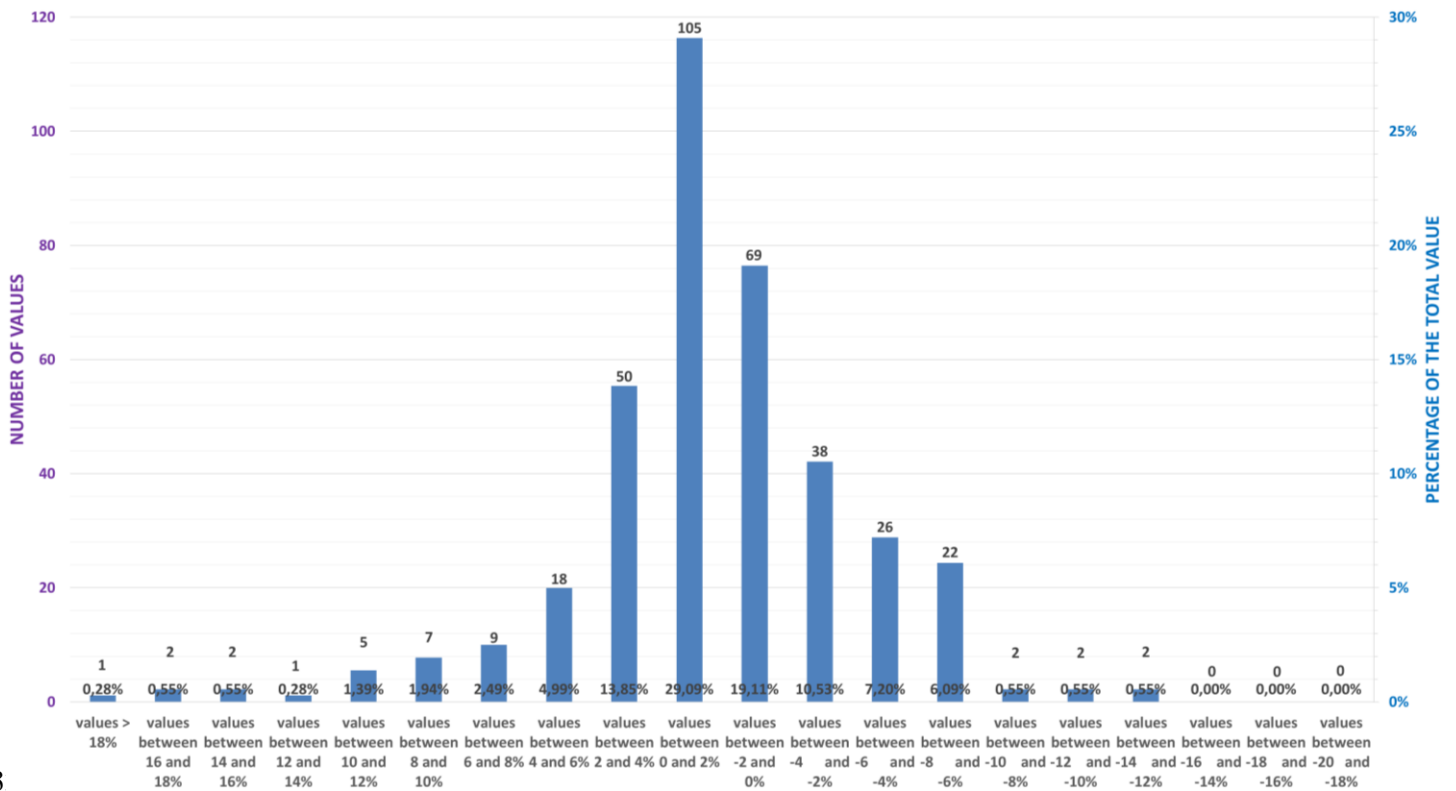


Figure 21 : Differences' repartition

3
336

IX. DISCUSSION

337

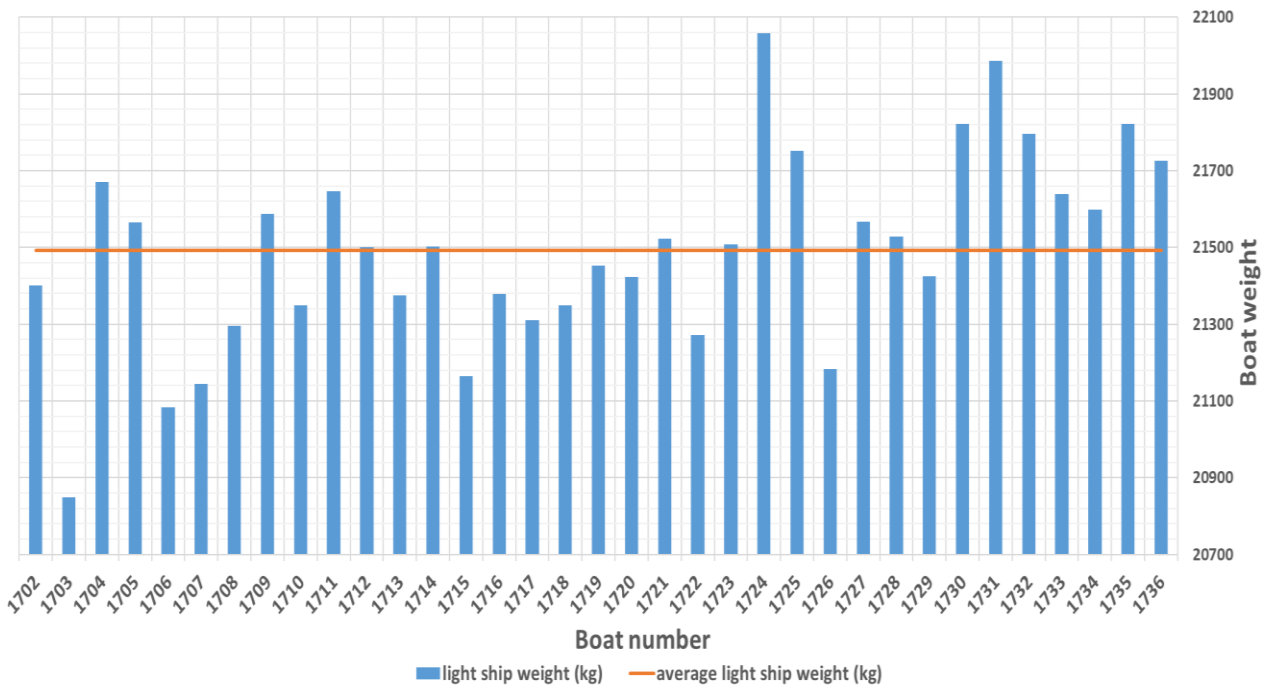
338 As demonstrated in the previous sections Savitsky's theory seems to be imprecise for $F_v < 0.9$ (~10.25 knots
 339 for the 1650 Plascoa). The improvements made in the current work leads to override this problem for the studied
 340 boat.

341 Another prediction has been made using the current PPT to estimate the top speed of a Couach's 12m boat
 342 called the WASP. The top speed found by calculation was 53 knots and the real top speed is 55 knots. The same
 343 study cannot be done for now because the boat is powered with outboard engines which are not equipped to
 344 measure the engine load / absorbed power.

345 This tool will be very useful in the next thesis work. It will permit to characterize the impact of an increased
 346 boat's mass and to study the influence the longitudinal position of the center of gravity.

347 For example, an inventory had been made on all the 35 boats light ship weight (see **Figure 22**).

348 According to this inventory the average light ship weight is 21493 kg, the maximum light ship weight is 22058
 349 kg and the minimum light ship weight is 20848 kg.



350

351

Figure 22 : inventory of light ship weight

352

The heavier boat is the number 24. It is 565 kg over the average light ship weight of the 35 boats. This added weight represents an increase of 2.63% from the average light ship.

354

These values have to be put into perspective because boats weight are measured by hydrostatic weighing. For this particular series of boat the total measure procedure can generate a maximum error of 400kg. If this measurement inaccuracy is masked, the boat is made of GRP (glass reinforced plastic) through the vacuum infusion method. This technique ensures an efficient industrial process but for technical reason the boat is not made of one piece and needs to be assembled. The assembling (stratification, gluing ...) process is highly operator dependent and represent 600 kg. Couach engineers have measured a 20% variability for this process which could lead to a changeability of 120 kg from boat to boat. More generally the Couach engineers have measured a 5% variability for all the composite work. As it represents about 6 tons of the boat it could lead to a changeability of 300 kg from boat to boat. Subcontractors too can generate weight error as they have their on weight tolerance.

364

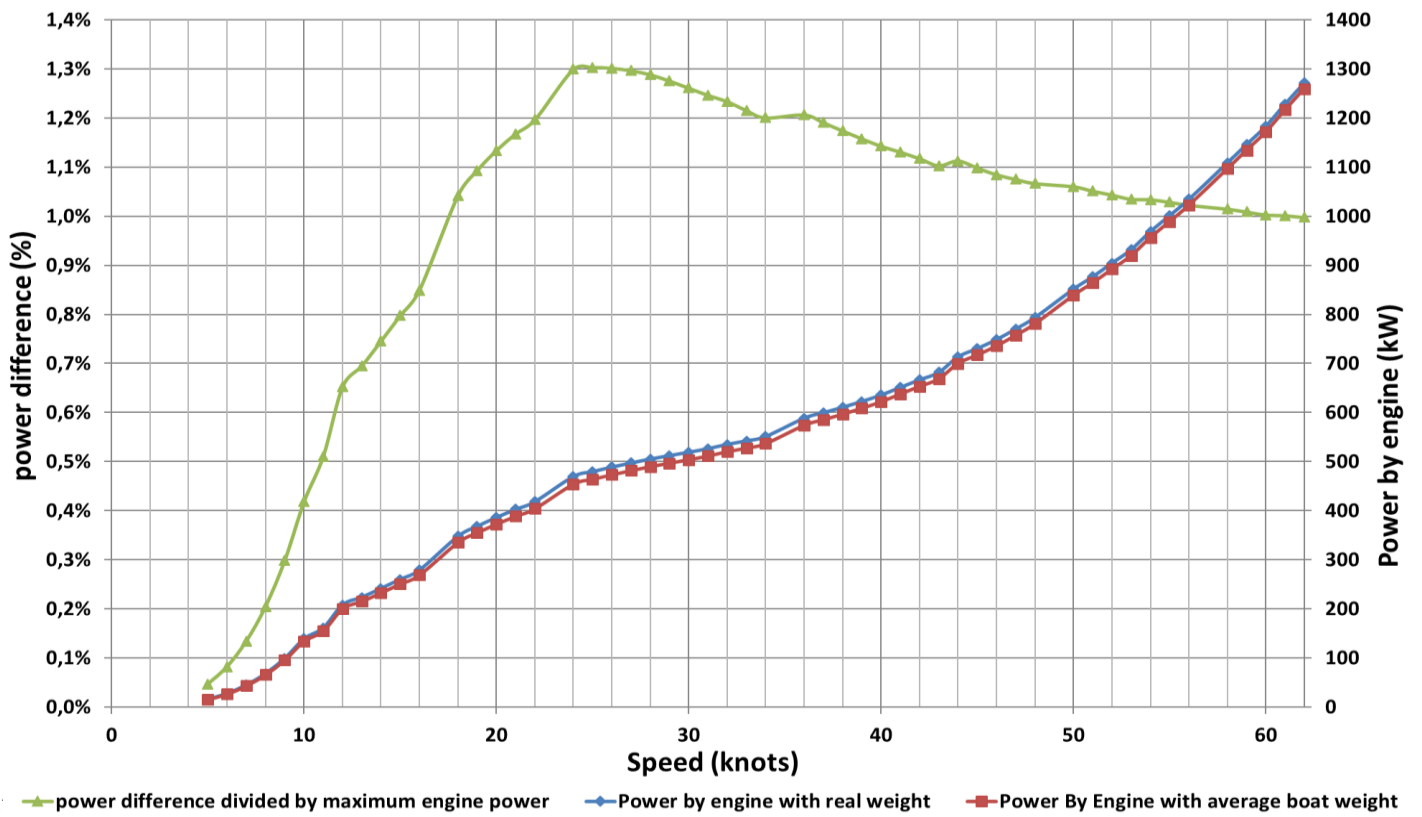
On the **Figure 23**, the absorbed power by engine, for the boat number 24 have been plotted, both with its real weight (blue curve) and with 565 kg less (red curve) to match with the boats average light ship weight. Then the two powers have been subtracted and divided by the maximum engine power (green curve). This green curve highlights the required overpower generated by the mass increased. On this

365

366

367

368 particular boat due to the mass increase of 2.63%, to maintain the boat full speed the engine need to deliver
 369 1% more power.



371 Figure 23 : study of a mass increase for a given boat

372

X. CONCLUSION

373

374 This study leads to validate the PPT, improved and calibrated with the input of measured data. Its precision is
375 quite surprising⁶ given the fact that it requires only few and easy to get parameters. The tool is fast executing and
376 easy to use. The code execution requires about 30 seconds to compute boat drag, required power, engine speed,
377 fuel consumption, boat range and endurance for 58 input speeds while on the same computer it takes about 24h
378 to compute the boat drag for only 1 input speed using a CFD code.

379 Some improvements could still be made for speed between 14 and 24 knots. They would modify locally the
380 Savitsky's theory as (**Blount, Fox, 1976**) did. And a CFD calculation or a wind tunnel test could validate the boat
381 Cx value of 1.1.

382 This tool will be very useful in the conception process at CNC, as well as for applied research purpose. It will
383 be used to characterize the impact of an increased boat's mass and to study the influence the longitudinal position
384 of the center of gravity.

⁶ All the 35 boats have been tested over a period of 11 month inside the Arcachon bay.

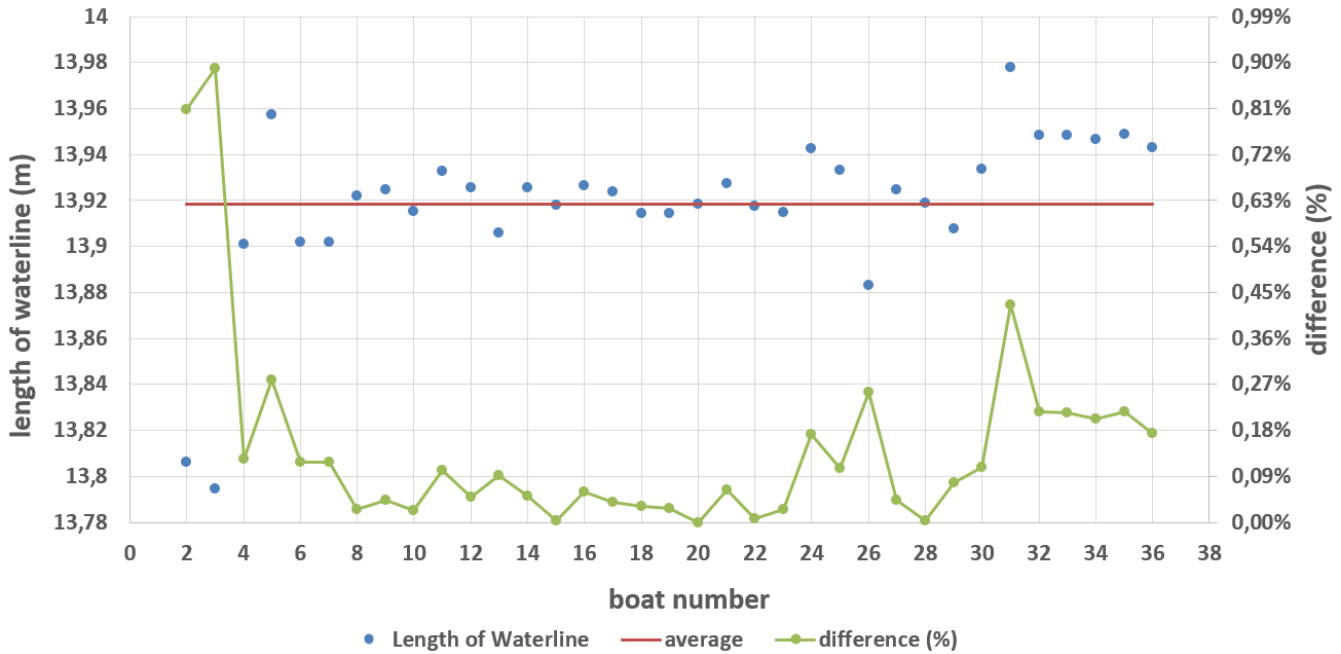
XI. REFERENCES

- 386 1. Angeli, J.C., April 1973. Evaluation of the Trim of a Planing Boat at Inception of Porpoising. The
387 Society Of Naval Architects And Marine Engineers. Paper presented at the Spring meeting, lake Buena
388 Vista, Florida.
- 389 2. Blount, D.L., Fox, D.L., January 1976. Small-Craft Power Prediction. Marine Technology, Vol. 13,
390 No. 1, pp. 14-45.
- 391 3. Caponnetto, M. Practical CFD simulations for planing hulls. Rolla Research.
- 392 4. Celano, T., 1998. The Prediction of Porpoising Inception for Modern Planing Craft. SNAME
393 Transactions, Vol. 106, pp. 269-292.
- 394 5. Cichowicz, J., Theotokatos, G., Vassalos, D., 2015. Dynamic energy modelling for ship life-cycle
395 performance assessment. Ocean Engineering 110 49–61.
- 396 6. Ekman, F., Naudo Ribas, C., Rydelius, F., May 2016. Model for Predicting Resistance and Running
397 Attitude of High-Speed Craft Equipped with Interceptors.
- 398 7. Lu, R., Turan, O., Boulougouris, E., Banks, C., Incecik, A., 2015. A semi-empirical ship operational
399 performance prediction model for voyage optimization towards energy efficient shipping. Ocean
400 Engineering 110 18–28.
- 401 8. Olivieri, A., Pistani, F., Avanzini, A., Stern, F., Penna R., September 2001. Towing Tank Experiments
402 Of Resistance, Sinkage And Trim, Boundary Layer, Wake, And Free Surface Flow Around A Naval
403 Combatant Insean 2340 Model. IIHR Technical Report No. 421.
- 404 9. Savitsky, D., October 1964. Hydrodynamic Design of Planing Hulls. Marine Technology.
- 405 10. Savitsky, D., DeLorme, M., Datla, R., January 2007. Inclusion of Whisker Spray Drag in Performance
406 Prediction Method for High-Speed Planing Hulls.
- 407 11. Sunny Verma., Shiju John, December 2010. Development of Correction Factors for improving Planing
408 Hull Performance Prediction. Conference Paper.
- 409 12. Svahn, D., June 2009. Performance Prediction of Hulls with Transverse Steps. Marina System Centre
410 for Naval Architecture.
- 411 13. Tezdogan, T., Demirel, Y.K., Kellett, P., Khorasanchi, M., Incecik, A., Turan, O., 2015. Full-scale
412 unsteady RANS CFD simulations of ship behaviour and performance in head seas due to slow steaming.
413 Ocean Engineering 97 186–206.
- 414 14. Turan, O., 2015. Energy efficient ship design and operations. Editorial Ocean Engineering 110.

415

XII. APPENDIX 1 : PPT INPUTS VARIATION RANGE

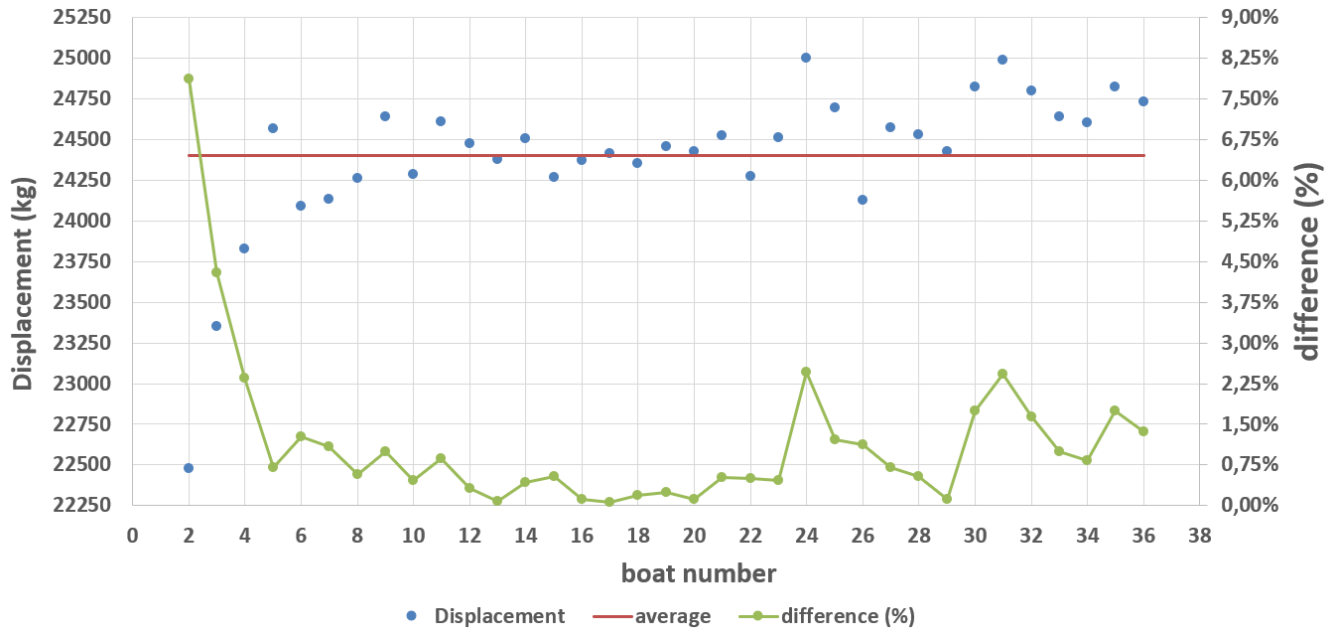
416 In this appendix the inputs variation range is presented with the four graph below. As a reminder the
417 specific data are length on waterline, beam at waterline, displacement and LCG.



419

Figure 24 : variation of the length of waterline for the 35 boats

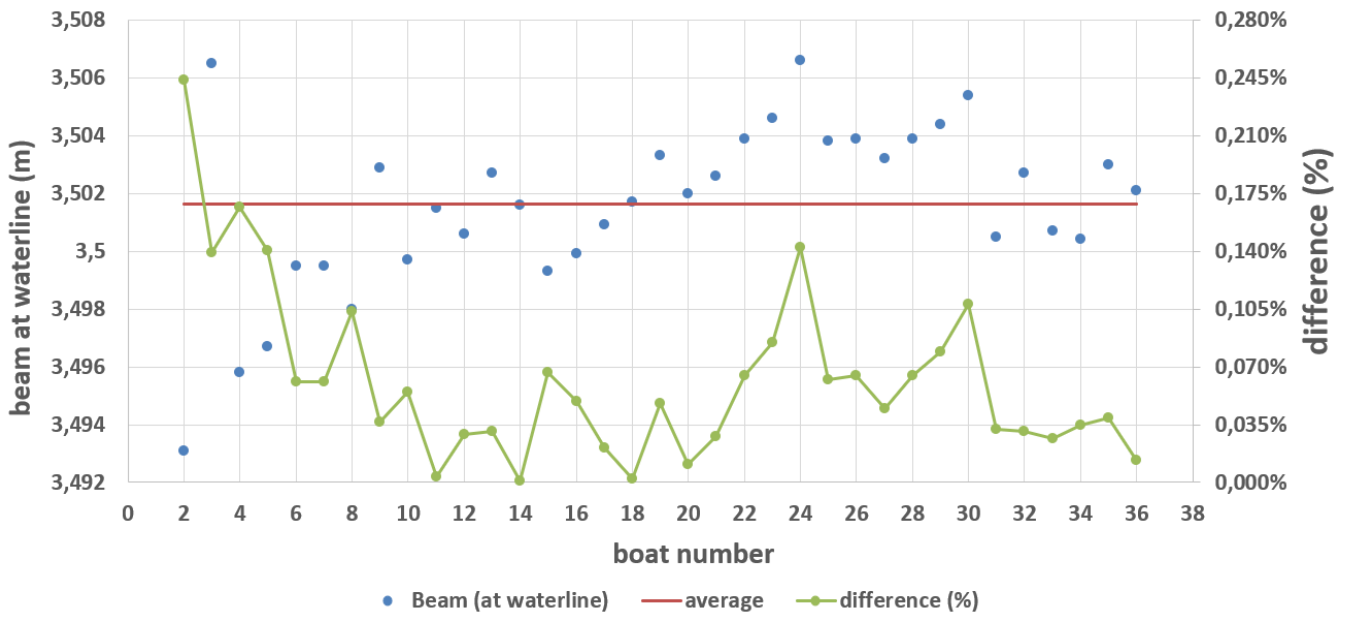
420



422
423

Figure 25 : variation of the displacement for the 35 boats

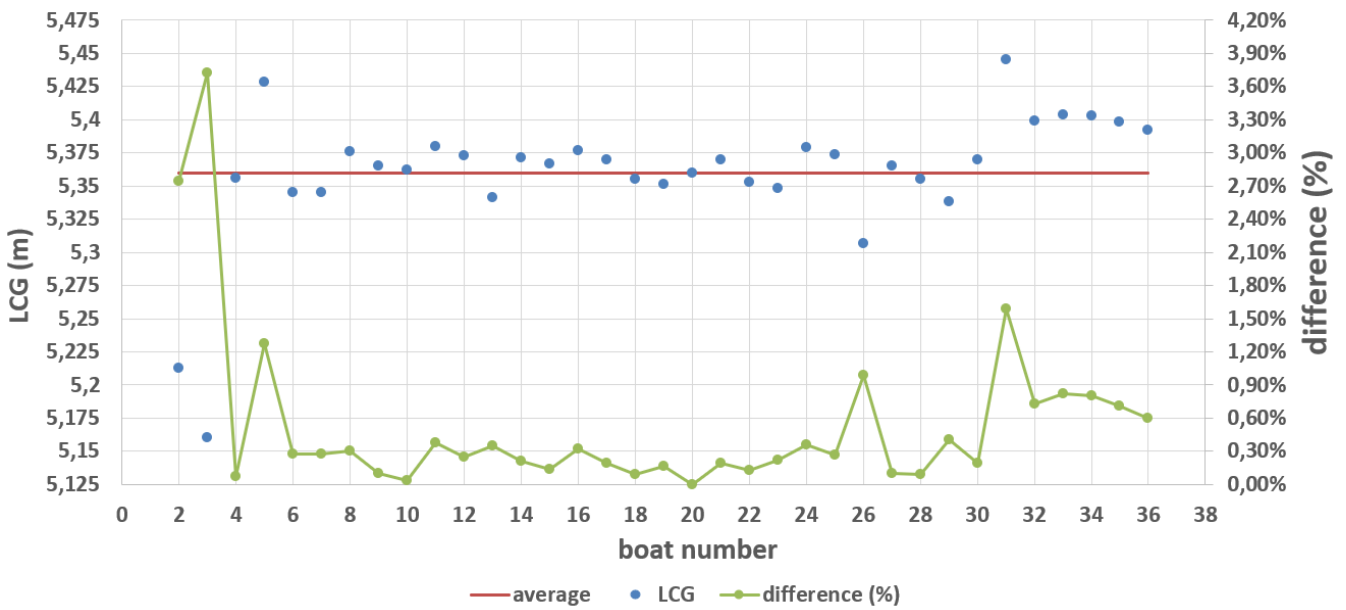
424



4
426

Figure 26 : variation of the beam at waterline for the 35 boats

427



4
429
430

Figure 27 : variation of the LCG for the 35 boats

431 **XIII. APPENDIX 2: SAVITSKY PROCEDURE LIMITATIONS AND**
432 **ASSUMPTIONS GIVEN BY EKMAN ET AL, 2016**

433 The following paragraph is directly extract from (Ekman et al, 2016) and gives limitations of the
434 Savitsky procedure.

435 *“The center of pressure is difficult to calculate, and two main assumptions need to be made. First of all,*
436 *the center of pressure of the dynamic component is said to be at 75 percent of the main wetted length*
437 *forward of the transom, and the buoyant force center of pressure at 33 percent also from the transom.*
438 *Another limitation of the Savitsky method is that equation (2.6) is only applicable for $0.60 \leq C_v \leq 13.0$, 2°*
439 *$\leq \tau \leq 15^\circ$ and $\lambda \leq 4$. These limitations comes from lambda being*

440
$$\lambda \leq \frac{Lw}{b},$$

441 *where the wetted length, Lw , is unlimited. This implies that the trim must be limited to a minimum of 2°*
442 *for lambda not to increase exponentially.”*